

Electronic Supporting Information

Smartphone-Assisted Urinary Methylmalonic Acid Sensing by an Imidazole-Based Probe via Analyte-Triggered Aggregation Mechanism

Bharat Kaushik^a, Ajeet Singh^a, Annu Agarwal^a, Nancy Punia^a, Inamur Rahaman Laskar^{a*}

Department of Chemistry, Birla Institute of Technology and Science, Pilani, Pilani Campus, Vidya Vihar, Pilani, Rajasthan 333031, India, Email: ir_laskar@pilani.bits-pilani.ac.in

Table of contents:

- Figure S1-S4. ¹H and ¹³C NMR of step-1 and step-2.
- Figure S5. HRMS spectra of M1.
- Figure S6. ¹H spectra of M1 in DMSO-d₆ solvent.
- Figure S7. Crystal structure of M1.
- Figure S8. Different angles of M1-MMA-M1 optimized structure.
- Figure S9. Emission spectra of M1 in different solvents.
- Figure S10. The excited state lifetime with the fitting parameter.
- Figure S11. Emission of M1 in methanol and water.
- Figure S12. Photograph of M1 under UV lamp (365 nm) with different components of Urine in the presence of MMA.
- Figure S13. Zeta potential distribution of M1 and M1-MMA.
- Figure S14. Jobs Plot for M1-MMA.
- Figure S15. PL spectrum of M1-MMA solutions with dilution.
- Figure S16. Time-dependent emission spectra of M1 in the presence of MMA.
- Figure S17. Emission spectrum of MMA sensing in a water: MeOH (9:1) solvent system.

1 **Figure S18.** Emission spectrum of M1(10 μ M) with different concentrations of MMA.

2 **Table S1.** Crystal Data Table of the crystal.

3 **Scheme S1.** Synthetic routes and molecular structures of M1 [(3,5-bis(4,5-diphenyl-1H-
4 imidazol-2-yl)-4-hydroxyphenyl) (phenyl) methanone].

5

6

7 **Experimental section**

8 **Materials and Instrumentation**

9 All the materials used were commercially available and were used without further purification.
10 The common salts (e.g., Ammonium acetate) were purchased from Merck. Milli-Q water was
11 used throughout this research work. UV-grade organic solvents were purchased from
12 Spectrochem and used without further purification. Deuterated chloroform and methanol were
13 purchased from Merck. ¹H NMR and ¹³C NMR spectra were recorded using a 400 MHz Bruker
14 NMR spectrometer. Mass spectra were recorded using an Agilent 6545 Q-TOF LC/MS, and
15 IR and UV-VIS absorption spectra were recorded using a Shimadzu Spectrophotometer (UV-
16 1800 and 2550). Steady-state photoluminescence (PL) spectra were recorded on a Horiba Jobin
17 Yvon Spectrofluorometer (FluoroMax-4). The quantum yield was measured by the Horiba
18 Fluoromax-Plus with a Quantaphi-2 integrating sphere. DLS and Zeta potential data were
19 recorded on Anton Paar LITESIZER 500. The single crystal was diffracted using a Rigaku
20 Oxford XtaLAB diffractometer. FEI: Apreo LoVac was used to record the FESEM imaging.
21 The four urine samples were collected from the BITS Medical Centre and handled according
22 to the method approved by the BITS Institutional Human Ethics Committee of the Birla
23 Institute of Technology and Science, Pilani, Pilani campus, Rajasthan (approval number
24 IHEC/BITS/A/02/20).

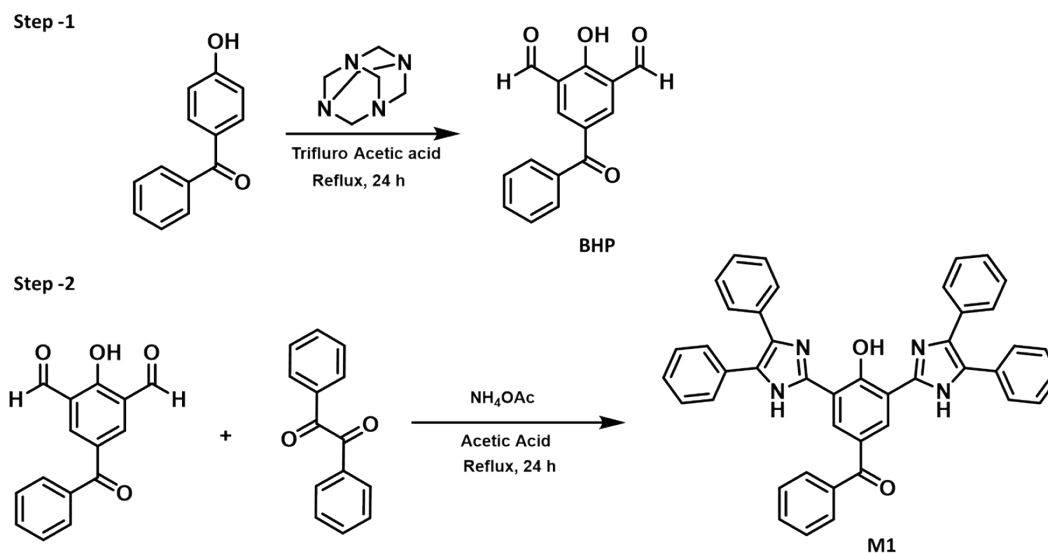
25

26 **Synthesis and characterization**

27 The fluorescent probe molecule M1 was synthesized and evaluated for its application in the
28 detection of methyl methacrylate (MMA). Structural characterization of the product was
29 carried out using NMR and IR spectroscopy, and the formation of M1 was further confirmed
30 by mass spectrometry. A single crystal was grown, and XRD analysis was also done. The probe

1 exhibited good solubility in polar organic solvents such as dichloromethane, tetrahydrofuran,
2 methanol, and dimethyl sulfoxide (DMSO).

3

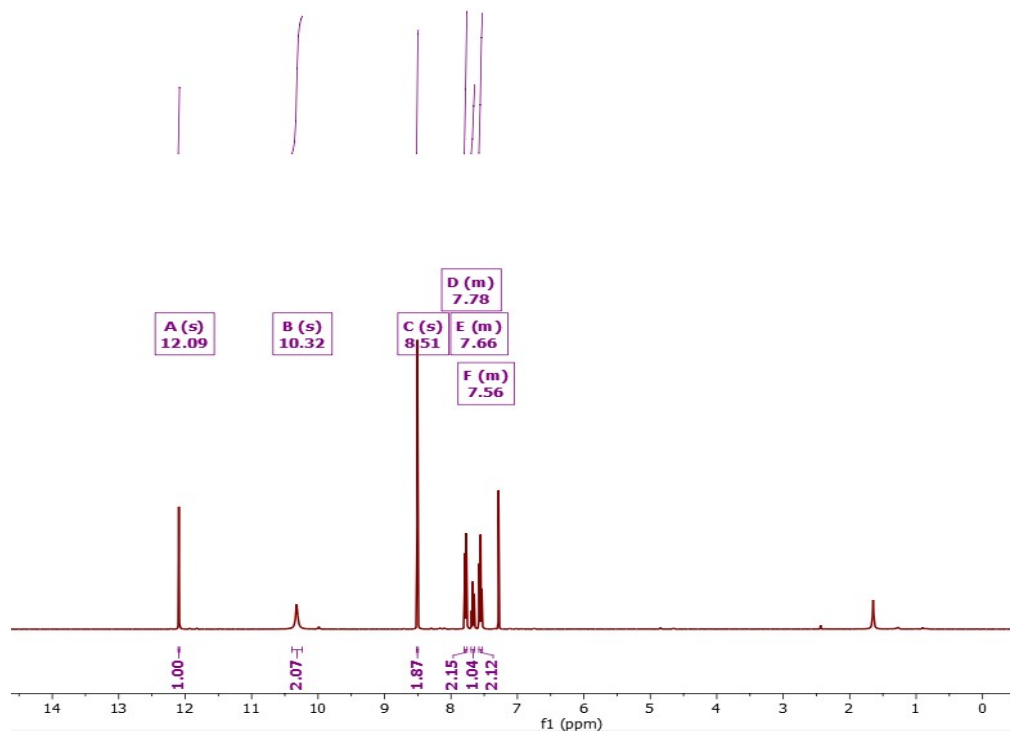


4

5

6 Scheme S1. Synthetic routes and molecular structures of M1 [(3,5-bis(4,5-diphenyl-1H-
7 imidazol-2-yl)-4-hydroxyphenyl) (phenyl)methanone].

8 ^1H NMR (400 MHz, Chloroform-*d*) δ 12.09 (s, 1H), 10.32 (s, 2H), 8.51 (s, 2H), 7.80 – 7.76
9 (m, 2H), 7.70 – 7.64 (m, 1H), 7.58 – 7.53 (m, 2H).



1

2

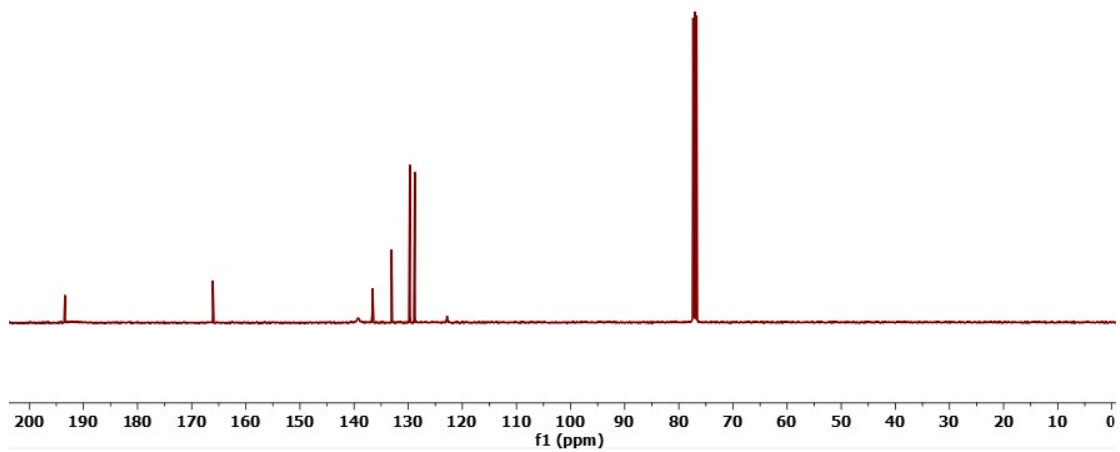
3 Figure S1: ¹H spectrum of 5-benzoyl-2-hydroxyisophthalaldehyde (BHP) in CDCl₃ solvent.

4

5

6

7 ¹³C NMR (101 MHz, Chloroform-d) δ 193.41, 166.09, 139.23, 136.58, 133.06,
 8 129.76, 129.70, 128.79, 128.70, 122.83.

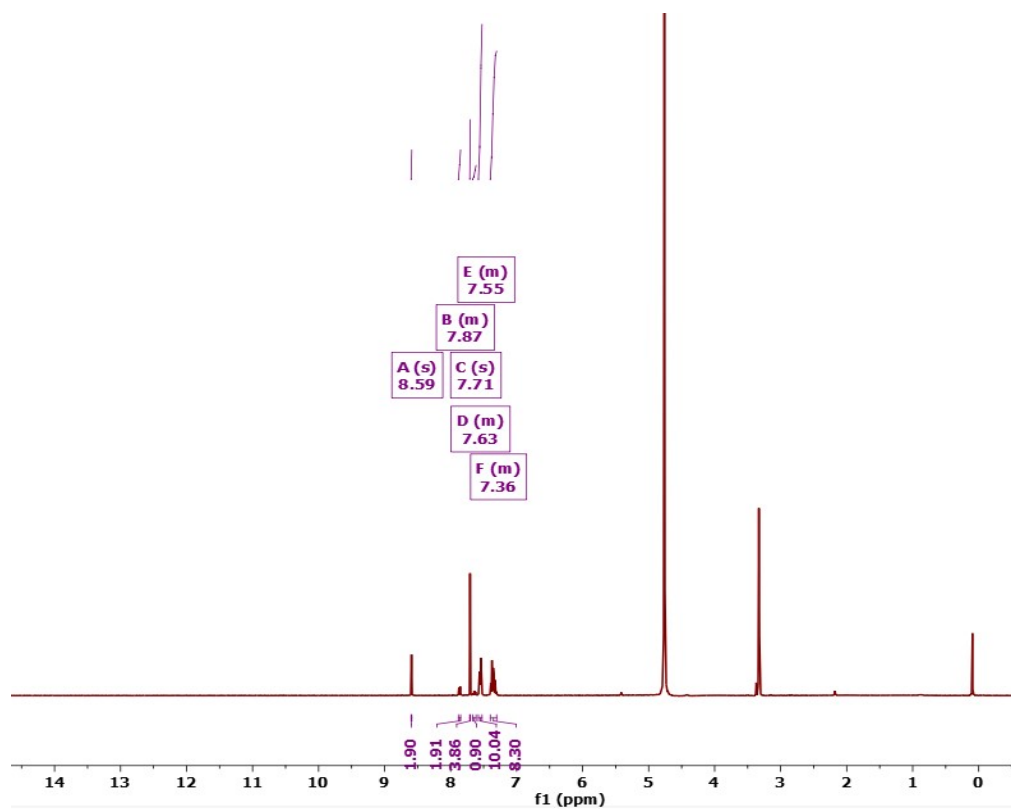


- 1
- 2
- 3
- 4
- 5
- 6
- 7
- 8
- 9
- 10
- 11
- 12
- 13
- 14
- 15
- 16

Figure S2: ^{13}C spectrum of 5-benzoyl-2-hydroxyisophthalaldehyde (BHP) in CDCl_3 solvent.

1
2
3
4
5
6
7
8
9
10
11
12

13 ^1H NMR (400 MHz, Methanol- d_4) δ 8.59 (s, 2H), 7.88 – 7.85 (m, 2H), 7.71 (s, 4H),
14 7.67 – 7.61 (m, 1H), 7.58 – 7.52 (m, 10H), 7.40 – 7.30 (m, 8H).

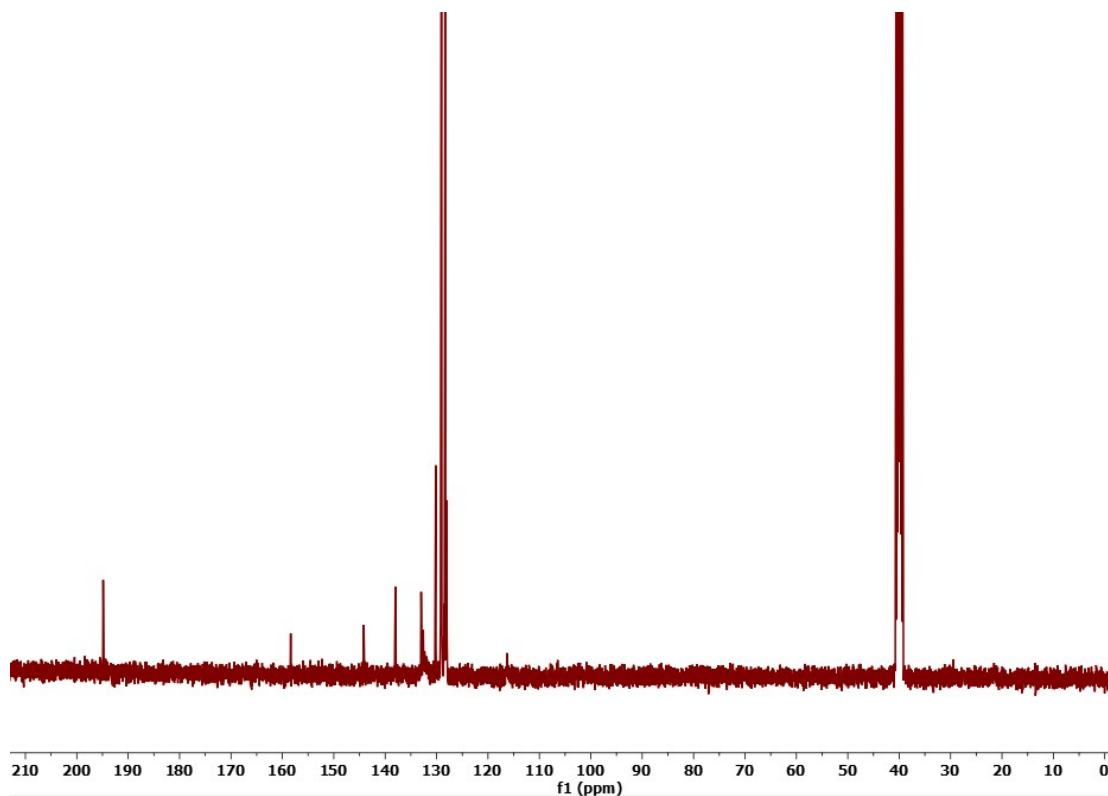


15
16
17
18
19

Figure S3: ^1H NMR spectrum of (3,5-bis(4,5-diphenyl-1H-imidazol-2-yl)-4-hydroxyphenyl)(phenyl) methanone (M1) in CD_3OD solvent.

1
2
3
4
5

^{13}C NMR (101 MHz, Chloroform-*d*) δ 194.87, 158.38, 144.16, 138.02,
133.01, 132.90, 132.60, 130.16, 129.24, 129.12, 129.04, 128.56, 128.35, 128.08, 116.19

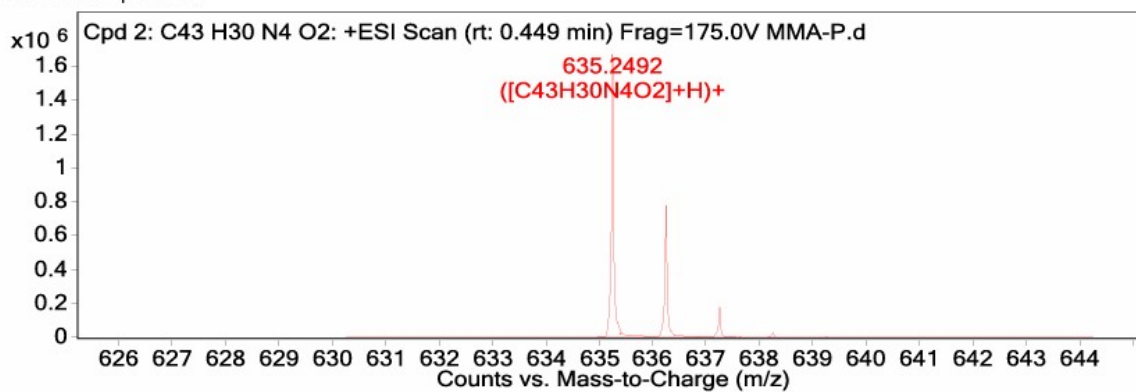


6

Figure S4: ^{13}C spectrum of compound (3,5-bis(4,5-diphenyl-1H-imidazol-2-yl)-4-hydroxyphenyl) (phenyl) methanone (M1) in CDCl_3 solvent.

7

MS Zoomed Spectrum

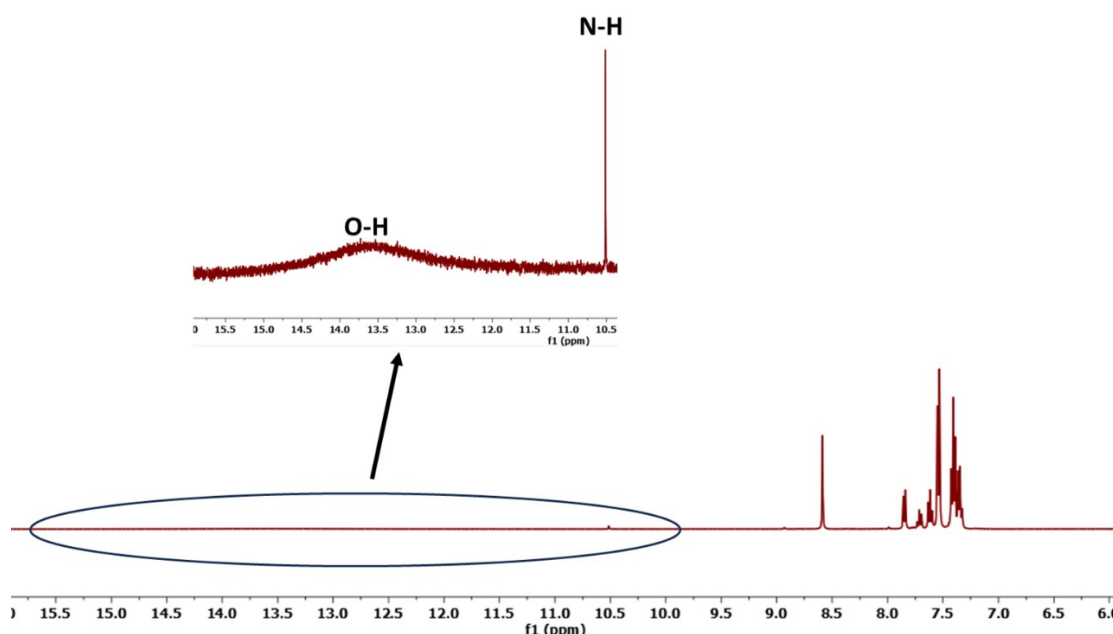


8

9

Figure S5: HRMS spectrum of compound M1.

1



2

3

4 Figure S6: ¹H NMR spectrum of (3,5-bis(4,5-diphenyl-1H-imidazol-2-yl)-4-hydroxyphenyl)
5 (phenyl) methanone (M1) in DMSO-d₆ solvent.

6 Preparation of Solutions

7 UV-grade methanol was used to prepare a 10⁻⁴ M stock solution of M1, while a 10⁻⁵ M aqueous
8 solution of methylmalonic acid (MMA) was prepared using Milli-Q water. For selectivity and
9 interference studies, aqueous solutions of various analytes commonly found in human urine
10 were similarly prepared in Milli-Q water, following the same procedure as for MMA.

11 Preparation of a chemically modified TLC strip

12 The circular-shaped 9 mm diameter TLC strip was used for testing. The TLC strip was
13 impregnated with 10⁻⁴M of the M1 probe and dried properly. After completely drying, different
14 concentrations of aqueous MMA were added to it and dried.

15 Computational details

16 The Density functional theory (DFT) was carried out using the Gaussian-16 package. To
17 consider the non-covalent interactions, a long-range corrected (LRC) hybrid functional, namely

1 ωB97XD. 6-31 G+ (d,p) was used as a basis set to incorporate polarization and diffusion
2 functions in the basis. The LRC functional was selected because the molecule exhibits charge-
3 transfer emission (as evidenced by **Figure S9**). Hybrid functionals like B3LYP are not well-
4 suited to account for non-covalent interactions; thus, it is necessary to use an LRC functional.
5 Further, we used the 6-31G+(d,p) double-zeta basis set, which includes diffuse and polarization
6 functions. This is because molecules contain electron-withdrawing atoms and lone pairs. The
7 same level of theory was used to perform time-dependent density functional theory (TDDFT)
8 to get insights into the excited state dynamics.

9 **Photophysical studies-**

10 A 10⁻⁴ M methanol solution of M1 was used for both absorption and emission measurements.
11 UV-Vis absorption spectra were recorded in the 200–800 nm range. Photoluminescence
12 spectra were recorded in the 350–650 nm range at an excitation wavelength appropriate for the
13 absorption maximum.

14 **Single-Crystal**

15 Single crystals of M1 were grown via slow evaporation of a hexane-layered dichloromethane
16 (DCM) solution. The well-formed, colorless, block-shaped crystals were obtained. A
17 transparent crystal of suitable quality was selected and analyzed using a Rigaku Oxford
18 XtaLAB diffractometer equipped with MoK α radiation ($\lambda = 0.71073 \text{ \AA}$). Data collection and
19 processing were carried out using CrysAlisPRO 2023, and structure solution and refinement
20 were performed using OLEX2 software in conjunction with SHELXT¹ (structure solution) and
21 SHELXL² (refinement) in Olex2-1.5³.

22 **Detection Limit Calculation**

23 The detection limit for MMA was evaluated via fluorometric titration using a 10⁻⁴ M methanol
24 solution of M1. Fluorescence intensity was recorded at various MMA concentrations, and a
25 calibration curve was generated by plotting the intensity against the analyte concentration. The
26 limit of detection (LOD) was calculated using the formula.⁴

27

$$28 \quad LOD = \frac{3\sigma}{K}$$

29 Where: σ = Standard deviation.

30 K = Slope obtained from the fluorescent intensity v/s analyte concentration plot.

1

2 **Quantum yield calculation**

3 To determine the absolute quantum yield, a 10^{-4} M methanol solution of M1 was utilized.

4 Quantum yield was measured using Fluoromax-Plus with a Quantaphi-2 integrating sphere.

5 The quantum yield of both MMA-containing (30 μ M) and MMA-free solutions were measured.

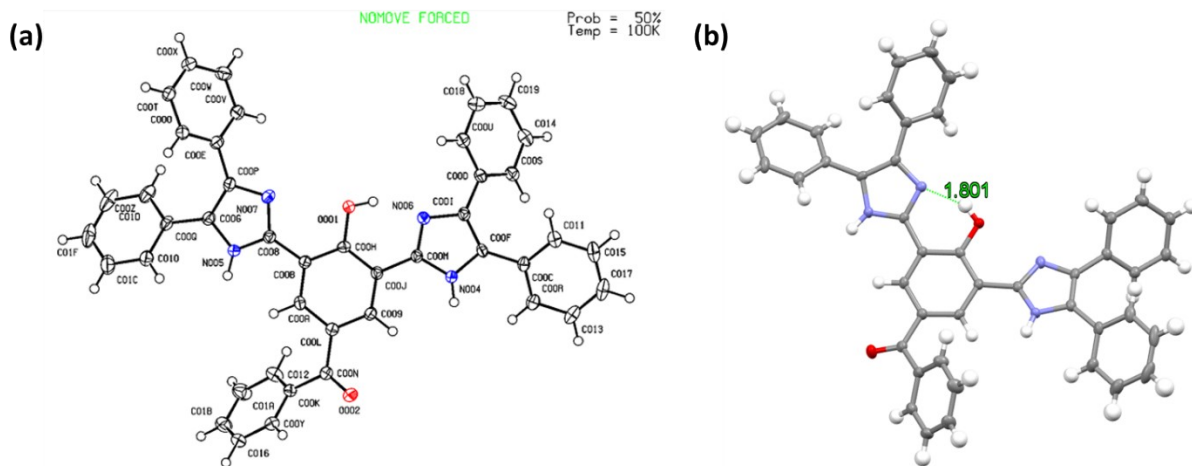
6

7 **Results and discussion**

8

9 **Single-Crystal Structure Analysis**

10 Single crystals of M1 were grown via slow evaporation of a hexane-layered dichloromethane
11 (DCM) solution. Well-formed, colorless, block-shaped crystals were obtained. A transparent
12 crystal of suitable quality was selected and analyzed using a Rigaku Oxford XtaLAB
13 diffractometer equipped with MoK α radiation ($\lambda = 0.71073$ Å). Data collection and processing
14 were carried out using CrysAlisPRO 2023, and structure solution and refinement were
15 performed using OLEX2 software in conjunction with SHELXT¹ (structure solution) and
16 SHELXL² (refinement) in Olex2-1.5³. Hydrogen atoms were refined isotropically, while all
17 non-hydrogen atoms were refined using the full-matrix least-squares method. The crystal
18 structure has been deposited with the Cambridge Crystallographic Data Centre (CCDC No.
19 2455842). Structural refinement revealed that the asymmetric unit contains one molecule.
20 Notably, an intramolecular hydrogen bond is observed between the hydroxyl proton of the
21 phenol group and the nitrogen atom of the benzothiazole ring, contributing to the molecule's
22 conformational stability.



1

2 Figure S7: (a) crystal structure of M1 crystal at 50% probability recorded at 100K; (b) H-
3 bond between OH and N atom of the ring with a bond distance of 1.801 Å.

4

5 Computational studies-

6

7

8

9

10

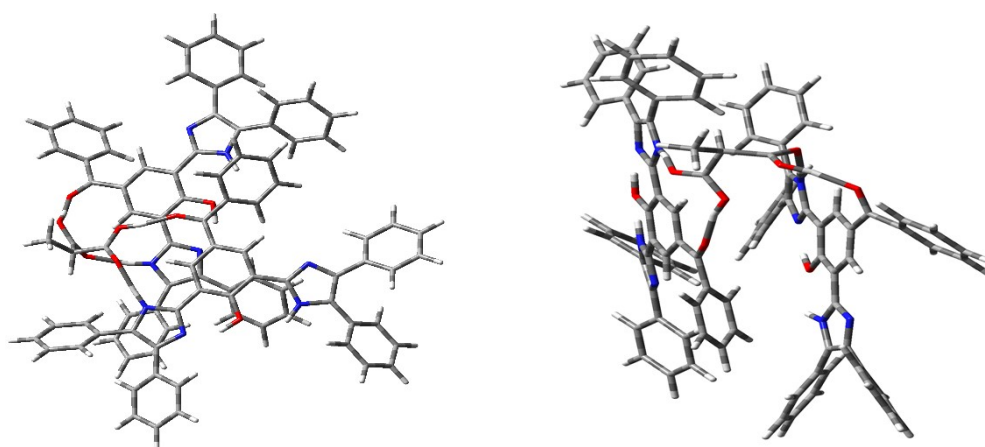
11

12

13

14

15



16 Figure S8: Different angle of optimized structure M1-MMA-M1.

17

18

19 Photophysical property study

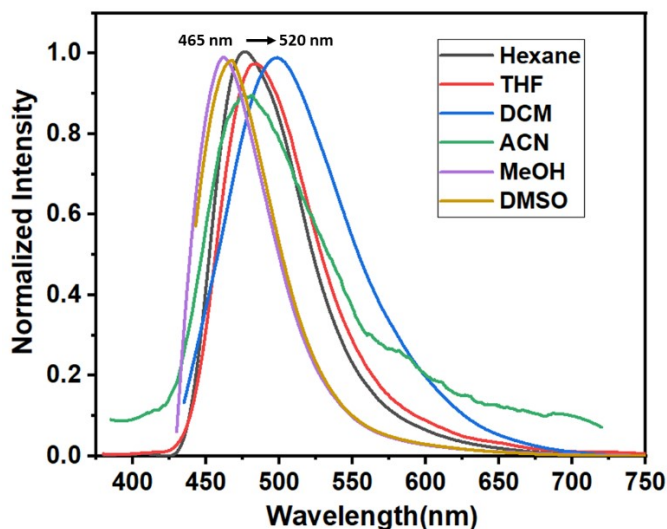
20

21

22

1

2



3

4

5 Figure S9: PL spectra in various solvents show a charge transfer (CT) character of M1 ($\lambda_{\text{ex}} =$
 6 310 nm) [Solvent with dielectric constant(k), Hexane (1.88), DCM (8.93), THF (7.58),
 7 Methanol (32.70), DMSO (46.68)].

8

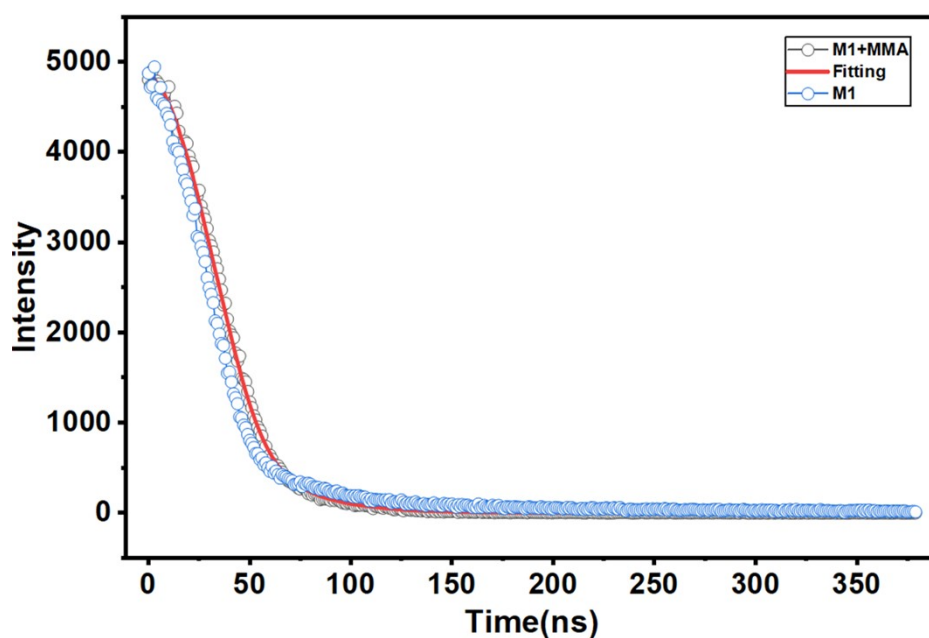
9 Table S1: Crystal Data Table of the crystal

CCDC No.	2455842
Empirical formula	$\text{C}_{47}\text{H}_{42}\text{N}_4\text{O}_4$
Formula weight	726.84
Temperature/K	100.15
Crystal system	triclinic
Space group	P-1
a/Å	9.4569(3)
b/Å	15.0362(4)
c/Å	15.0481(5)
$\alpha/^\circ$	62.286(3)
$\beta/^\circ$	81.041(3)
$\gamma/^\circ$	87.675(2)
Volume/Å ³	1869.95(11)
Z	2
$\rho_{\text{calc}}/\text{cm}^3$	1.291
μ/mm^{-1}	0.083
F(000)	768.0
Crystal size/mm ³	0.125 × 0.03 × 0.02
Radiation	MoK α ($\lambda = 0.71073$)
2 Θ range for data collection/ $^\circ$	4.364 to 52.388

Index ranges	$-7 \leq h \leq 11, -18 \leq k \leq 18, -18 \leq l \leq 18$
Reflections collected	24254
Independent reflections	6965 [$R_{\text{int}} = 0.0303, R_{\text{sigma}} = 0.0385$]
Data/restraints/parameters	6965/0/444
Goodness-of-fit on F^2	1.096
Final R indexes [$I \geq 2\sigma(I)$]	$R_1 = 0.0436, wR_2 = 0.1227$
Final R indexes [all data]	$R_1 = 0.0560, wR_2 = 0.1297$
Largest diff. peak/hole / $e \text{ \AA}^{-3}$	0.64/-0.68

1

2 Time-resolved PL spectroscopy-



3

4

Compound	B1	B2	$\langle \tau \rangle$ (ns)	χ^2	Quantum Yield
M1	93.21	6.79	0.14	1.002	0.07
M1 + MMA	100	0	0.11	1.004	0.51

5

Figure S10: For M1 bi-exponential (components B1 and B2) and M1 + MMA mono-exponential decay, fitting was observed in methanol solvent. The excited state lifetime with the fitting parameter is shown in the table.

6

1 M1 probe Emission in Methanol and Water

2
3
4
5
6
7
8
9
10
11
12
13

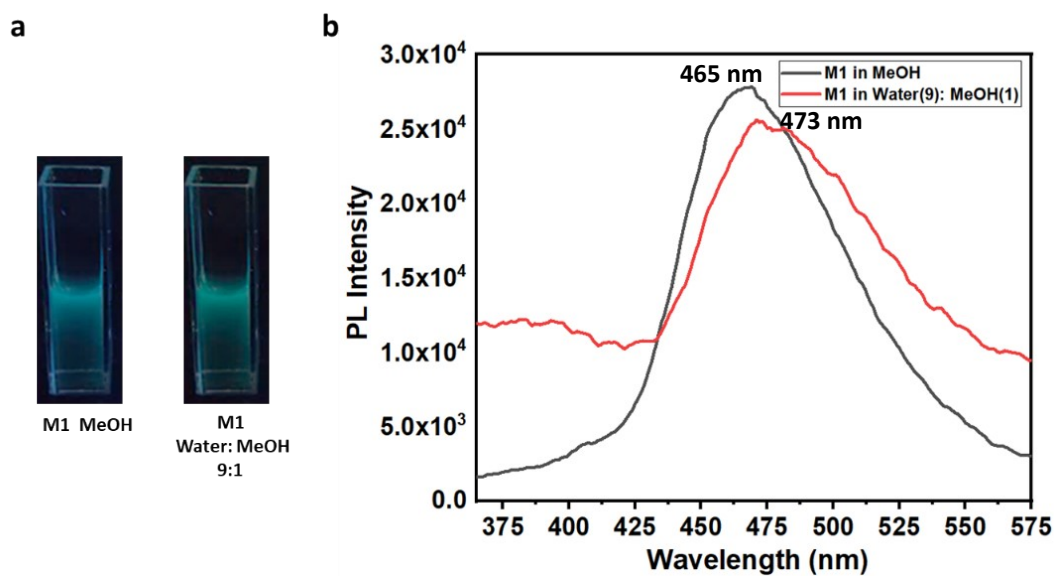


Figure S11: (a) Photograph of methanol and methanol water mixture solution of M1 under UV lamp (365 nm), (b) PL spectra of both solutions at 310 nm excitation.

14
15
16
17
18
19



Figure S12: Photograph of M1 under UV lamp (365 nm) with different components of Urine in the presence of MMA.

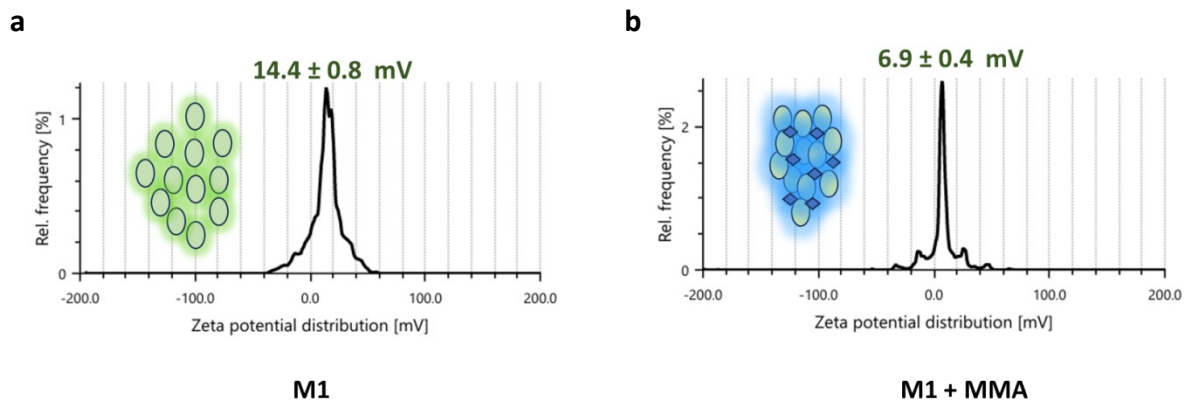
20
21
22
23
24
25
26

1

2

3 Zeta Potential

4



12 Figure S13: Zeta potential distribution of M1 and M1-MMA.

13

14

15

16

17 Job's Plot

18

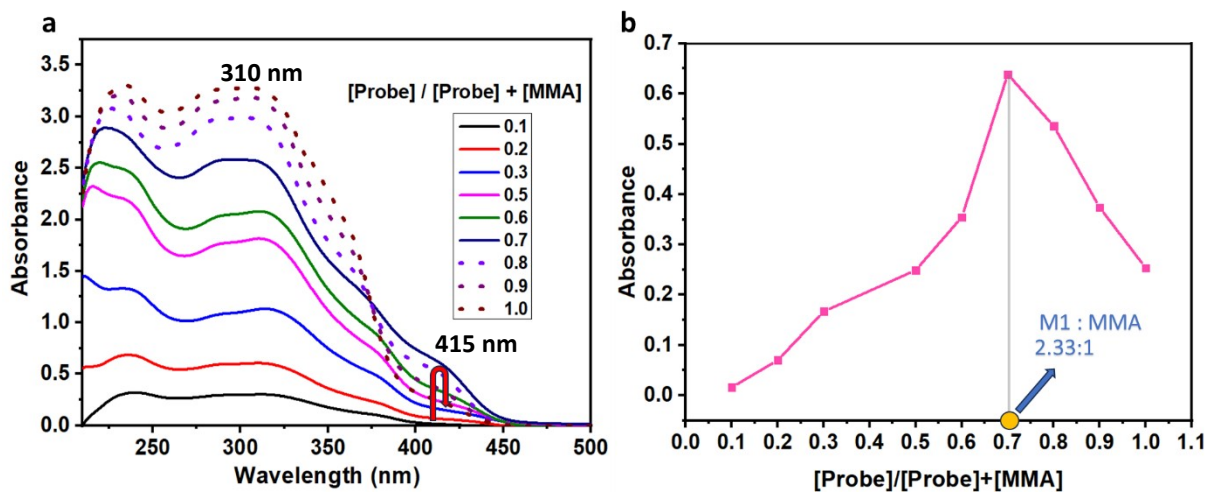
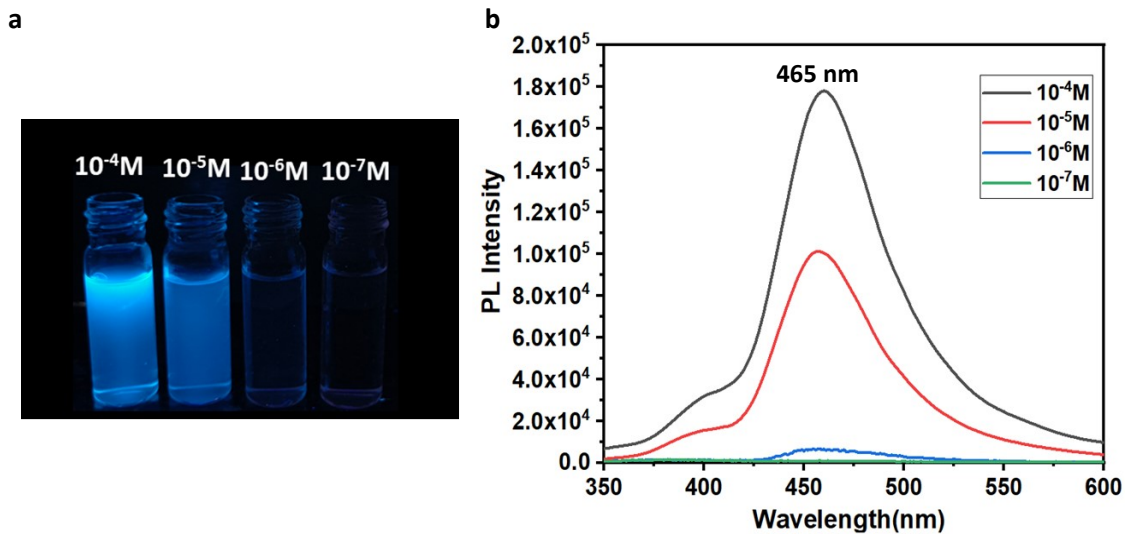


Figure S14: (a) UV-visible spectra of M1 probe with different ratios of probe and MMA for Job's plot [at 415 nm, up to 0.7 ratio, absorption increases (solid line), after that, it decreases (dotted line)]; (b) Job's plot of M1 probe in MeOH with aq. MMA (at 415 nm)

27

28

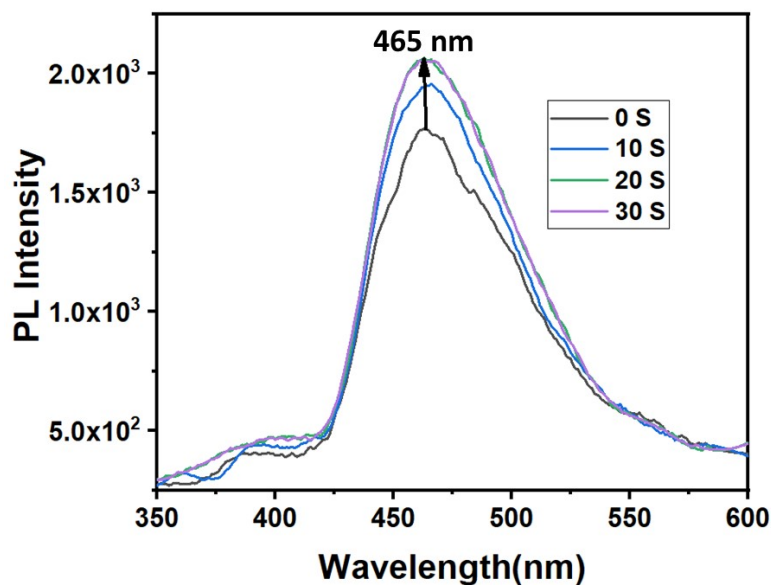
1
2
3
4
5
6
7
8
9
10
11
12
13



14 Figure S15: (a) Image of M1-MMA mixture with dilution under UV lamp (365 nm), (b) PL
15 spectrum of the same M1-MMA solutions ($\lambda_{ex} = 310$ nm).

16
17
18
19
20
21
22
23
24
25
26
27
28

Time-dependent study



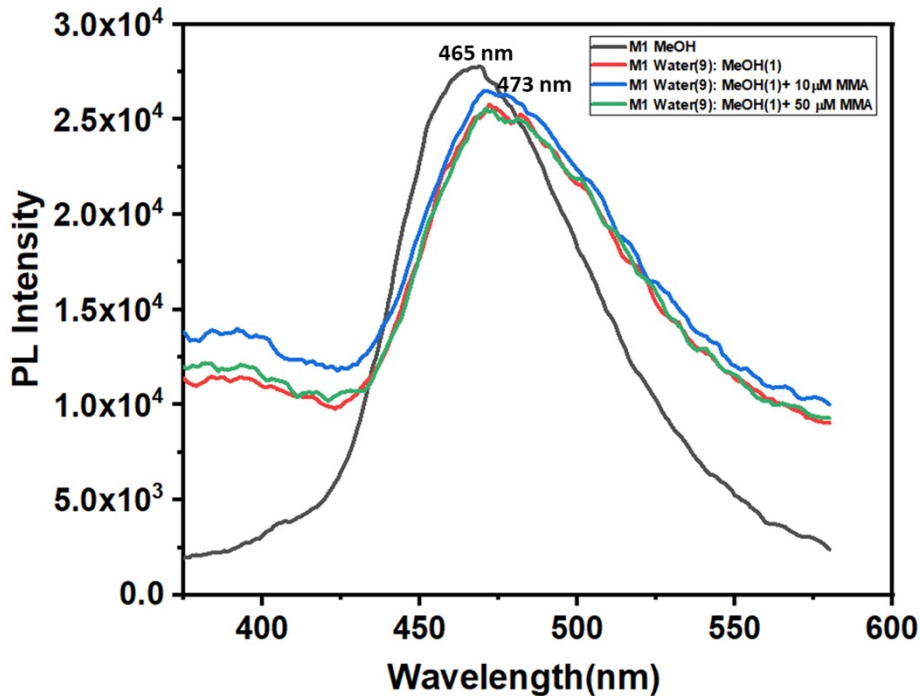
1

2 Figure S16: Time-dependent emission spectra of M1 (10^{-4} M in MeOH) in the presence of 10
 3 μM of MMA at room temperature (25°C).

4

5

6



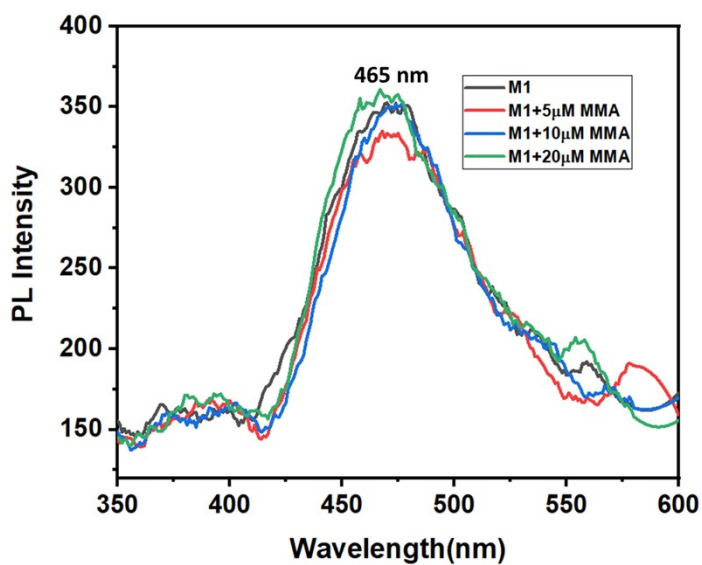
7

8 Figure S17: Emission spectra of MMA sensing in water: MeOH (9:1) solvent system.

9

10

1



2

3 Figure S18: Emission spectrum of M1 (10 μ M) with different concentrations of MMA.

4

5

6

7

8

9

10

11

12

13

14

15

16

17 **References: -**

18

- 19 1. G. Sheldrick, *Acta Crystallographica Section A*, 2015, **71**, 3-8.
- 20 2. G. Sheldrick, *Acta Crystallographica Section C*, 2015, **71**, 3-8.
- 21 3. O. V. Dolomanov, L. J. Bourhis, R. J. Gildea, J. A. K. Howard and H. Puschmann, *Journal of*
- 22 *Applied Crystallography*, 2009, **42**, 339-341.
- 23 4. D. A. Armbruster and T. Pry, *The Clinical biochemist. Reviews*, 2008, **29 Suppl 1**, S49-52.

